ESCUELA DE CONSTRUCCIÓN CIVIL
FACULTAD DE INGENIERÍA

Revista de la Construcción
Journal of Construction

Research Article

Experimental evaluation of the usability of palm tree pruning waste (PTPW) as an alternative to geotextile

Ebubekir Kaplan[1], Cafer Kayadelen[2], Mitat Öztürk[3, *], Yakup Önal[4], Gökhan Altay[5]

[1] Osmaniye Korkut Ata University, Faculty of Engineering, Department of Civil Engineering, Osmaniye (Turkey), ebubekirkaplan58@gmail.com

[2] Osmaniye Korkut Ata University, Faculty of Engineering, Department of Civil Engineering, Osmaniye (Turkey), ckayadelen@osmaniye.edu.tr

[3] Osmaniye Korkut Ata University, Faculty of Engineering, Department of Civil Engineering, Osmaniye (Turkey), mitatozturk@osmaniye.edu.tr

[4] Osmaniye Korkut Ata University, Faculty of Engineering, Department of Civil Engineering, Osmaniye (Turkey), yakuponal@osmaniye.edu.tr

[5] Osmaniye Korkut Ata University, Faculty of Engineering, Department of Civil Engineering, Osmaniye (Turkey), gokhanaltay@osmaniye.edu.tr
*Correspondence: mitatozturk@osmaniye.edu.tr

Received: 18.06.2021; **Accepted:** 21.03.2022; **Published:** 18.04.2022

Citation: Kaplan, E., Kayadelen, C., Öztürk, M., Önal, Y. and Altay, G. (2022). Experimental evaluation of the usability of palm tree pruning waste (PTPW) as an alternative to geotextile. Revista de la Construcción. Journal of Construction, 21(1), 69-82. https://doi.org/10.7764/RDLC.21.1.69.

Abstract: This paper focuses on serving twofold benefits for the environment by providing not only recycling of a waste material but also improving rutting performance of sand subgrade under cyclic traffic loads. In this context, a series of laboratory experiments have been conducted to benchmark the performance of commercially manufactured geotextile and palm tree pruning waste (PTPW) as soil improvement agents. Experimental results of the study were evaluated based on permanent (plastic), total, and elastic deformation, rut depth reduction (RDR), traffic benefit ratio (TBR), percentage of elastic deformation, and resilient modulus (M_R). In the view of experimental results, geotextile and PTPW-reinforced sand subgrades demonstrated well performance in the sense of permanent and elastic deformations when compared to unreinforced case. It is also realized that the most satisfactory performance was obtained when geotextile or PTPW are located at a burial depth of both 50 mm and 100 mm. In that case, TBR values of geotextile and PTPW-reinforced subgrades were almost the same at 20 mm permanent deformation (i.e., 6.71 and 6.76, respectively). Furthermore, when the results were evaluated based on RDR, it is observed that geotextile and PTPW reinforcements reduced the rut depth at the rate of 49.31 % and 37.15 % at the end of 5000 load cycle, respectively.

Keywords: palm tree pruning waste, geotextile, soil stabilization, resilient modulus (M_R), recycling waste materials.

1. Introduction

When considering a highway pavement system, dynamic traffic loads ought to be effectively distributed from the upper layers of the pavement system to the downward, i.e., eventually to the subgrade. Furthermore, the subgrade layer of the pavement system should bear the distributed traffic loads; otherwise, it will be inevitable that pavements can suffer from typical distresses such as rutting which is one of the most undesirable distress types. To prevent this distress, layer thickness of the base and/or subbase can be increased; thus, dynamic traffic loads are allowed to be distributed over a larger area.

Besides, replacing weak subgrade with high-quality soil which is an expensive and inconvenient method can be thought of as another way of avoiding this phenomenon. Apart from these, stabilization of the subgrade can be considered to be a more convenient method. In literature, several stabilization methods such as geosynthetics, fibers, and additives (i.e., cement, lime, fly ash, and bitumen, etc.) for improving the bearing capacity of subgrade have been introduced (Basha, Hashim, Mahmud, & Muntohar, 2005; Fannin & Sigurdsson, 1996; Gray & Ohashi, 1983; Shukla, 2002). Among these methods, it can be said that geosynthetics are the most common and popular product for soil stabilization (Hausman, 1987; Fannin & Sigurdsson, 1996; Giroud & Han, 2004; Kayadelen, Önal, & Altay, 2018; Altay, Kayadelen, Taşkıran, & Kaya, 2019; Negi & Singh, 2019; Altay, Kayadelen, Taskiran, Bagriacik, & Toprak, 2021; Altay, Kayadelen, Canakci, Bagriacik, Ok, & Oguzhanoglu, 2021).

The use of geosynthetics for stabilizing subgrade and reinforcing the base layer of unpaved roads and areas have been date back to the 1970s (Giroud & Han, 2004). Geotextile, geogrid, and geocell are the most commonly used type of geosynthetics. One of these three types of geosynthetics, geotextile is generally used as a separator between subbase or base layer and subgrade; accordingly, a potential decrease in the bearing capacity of the subgrade due to the intermixing of coarse subbase or base material and fine subgrade material (i.e., contamination of the coarse subbase or base material with subgrade fines) can be prevented. Furthermore, the use of geotextile between the interface of the subgrade and subbase or base layer also provides traffic loads to be distributed over a larger area; therefore, it is enabled that bearing capacity of the subgrade is increased. In other words, geotextile is deflected by the traffic load and more tension force is generated; therefore, vertical component of this force in the geotextile contributes to decreasing the pressure on the subgrade. This mechanism of geotextile is called as membrane effect (Hausmann, 1987; Zhang, Zhao, Shi, & Zhao, 2010) and illustrated in Figure 1.

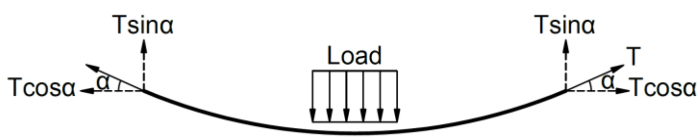

Figure 1. Membrane effect of geotextile reinforcement (modified from Zhang, Zhao, Shi, & Zhao, 2010).

It is undeniable fact that geosynthetics have an advantage in reducing not only highway base layer thickness but also improving the rutting performance of the pavement systems (Önal, 2021; Suku, Prabhu, Ramesh, & Babu, 2016); thus, geosynthetics also enable the construction cost to decrease considerably. Moreover, with the help of decreasing the base layer thickness, geosynthetics provide an opportunity both to reduce excessive demand for natural aggregates causing to loss of natural resources and to reduce stone quarrying and crushing activities which harm not only the environment but also human health (Mandal & Pal, 2020). In literature, there is a variety of experimental studies related to the investigation of the use of geosynthetics as a reinforcement agent in road embankments(Cuelho & Perkins, 2017; George, Banerjee, Puppala, & Saladhi, 2021; Mamatha & Dinesh, 2019; Nair & Latha, 2016; Negi & Singh, 2019; Pokharel, Han, Leshchinsky, & Parsons, 2018; Pokharel, Han, Leshchinsky, Parsons, & Halahmi, 2010; Rashidian, Naeini, & Mirzakhanlari, 2018; Saride, Rayabharapu, & Vedpathak, 2015; Singh, Trivedi, & Shukla, 2019). According to the experimental results of these studies, when geosynthetics used as reinforcement, it was obviously observed that geosynthetics enhanced the performance of the reinforced layers.

Apart from the commercially manufactured geosynthetics, natural reinforcement materials have been gaining significance because these materials have twofold benefits for a cleaner and sustainable environment. In other words, the use of waste material as a reinforcement agent enables both to recycle a waste material, which is so trouble not only to store but also to destroy, and to improve rutting performance. Evangeline, Sayida & Girish (2019) conducted a field study on five different road sections to investigate the long-term performance of the rural roads reinforced with coir geotextile located at the interface of the subgrade or subbase and base course layer. They carried out dynamic cone penetration, Benkelman beam deflection, and field California bearing ratio tests on five coir geotextile-reinforced roads and compared their performance with the unreinforced case. They observed that lower dynamic cone penetration index values are obtained for reinforced sections than unreinforced one, and these index values decrease in the range of 25 % and 80 %. Furthermore, researchers noted that reinforced sections have higher value of field CBR than the unreinforced case, and from 22 % to 178 % increase in the field CBR values is attained. They also concluded that based on the Benkelman beam deflection test results, reinforced sections showed reduction in the characteristic deflection. Bhattacharyya, Fullen, Davies & Booth (2009) explored the effect of palm-leaf geotextile mats on conserving soil and reducing erosion. After one year of field experiments, they discovered that with the application of palm mats on unreinforced case, the soil splash height and splash erosion were decreased by 51 % and 90 %, respectively.

In this study, it was aimed to investigate the potential use of PTPW as an alternative to commercially manufactured geotextile. The palm tree used in the experiments is known as the Mexican fan palm (i.e., Washingtonia robusta). Palm trees some species of which is able to be in the range of 150 and 300 hundred years are pruned for removal of old leaves and for bloom at least once a year. Therefore, this pruning generates massive amount of biomass that has generally been discarded at garbage dump sites or has been burnt which is so harmful for environment (Ferrández-García, Ferrández-García, Ferrández-Villena, Hidalgo-Cordero, García-Ortuño & Ferrández-García, 2018). Furthermore, the pruning activity of Washingtonia robusta, which grows very fast generates, waste as 35.70 kg/tree annually (Garcia-Ortuno, Ferrandez Garcia, Andreu Rodriguez, Ferrandez Garcia, & Ferrandez-Villena, 2011).

Considering that this amount of waste belongs to one tree, the huge amount of waste material generated by pruning activity needs to be utilized for a sustainable and cleaner environment. In this regard, some researchers spread on a great effort to recycle PTPW material in the field of civil engineering (Abdeldjouad, Asadi, Ball, Nahazanan, & Huat, 2019; Arifin & Rahman, 2019; Marandi, Bagheripour, Rahgozar, & Zare, 2008; Mujah, Rahman, & Zain, 2015; Nnochiri, Ogundipe, & Oluwatuyi, 2017; Pourakbar, Asadi, Huat, & Fasihnikoutalab, 2015; Qu & Xiong, 2020; Qu & Zhao, 2016; Qu & Zhu, 2021). In their study, Gil-Lopez, Medina-Molina, Verdu-Vazquez & Martel-Rodriguez (2017) utilized fragmented PTPW with soil in different combinations as a percentage to construct an eco-friendly roadside noise barrier and used water as binding element. They obtained the most satisfactory result in the combination of 50 % chippings and 50 % soil for sound absorption. They also conducted an economic analysis to compare the costs of this recycled noise barrier with the cost of a noise barrier made from conventional materials like wood, cement, aluminum, and acrylic.

In the light of the economic analysis, they emphasized that the cost of the recycled noise barrier per meter square is approximately half of the conventional ones as well as being eco-friendly. Mujah, Rahman & Zain (2015) investigated the potential reusability of the ground palm oil fuel ash (POFA) to reinforce soft soil. They found that the cohesion values and internal friction angles of soft soil are increased at the rate of 60 % and 50 %, respectively when reinforced with ground POFA. They also noted that in the case of using a smaller particle size of POFA rather than the larger particle size, the improvement factor is more dominant; furthermore, in the event of the soil sample is fully saturated, they also observed a similar trend in the consolidation results. Nnochiri, Ogundipe & Oluwatuyi (2017) examined the influence of palm kernel shell ash (PKSA) on lime-stabilized clay soil. They observed an increase in CBR values and a decrease in both liquid limit and plasticity index with the addition of PKSA and lime to clay. Qu & Zhu (2021) performed unconfined compressive tests in order to investigate the mechanical properties of clayey soil reinforced with palm fiber of various contents and lengths. They found that energy adsorption capacity, strength, and ductility of reinforced clayey soil enhanced with the addition of palm fiber. They also stated that the energy adsorption capacity of reinforced clayey soil is enhanced by 580 % with palm fiber for samples with a content of 0.4 % and a length of 15 mm compared to unreinforced clayey soil.

In the current study, a comparative study was carried out to investigate the usability of PTPW as an alternative to commercially manufactured geotextile. In this context, seven laboratory model tests were conducted on sand subgrade reinforced with geotextile and PTPW with different configurations under cyclic loads. In addition, experimental results were evaluated based on permanent, total, and elastic deformation, TBR, RDR, percentage of elastic deformation, and M_R.

2. Materials and methods

2.1. Subgrade material

In all experiments, poorly graded sand (SP) which is determined according to the Unified Soil Classification System (USCS) was used. The grain size curve of the subgrade material is shown in Figure 2. Properties of the sand used in the experiments are presented in Table 1.

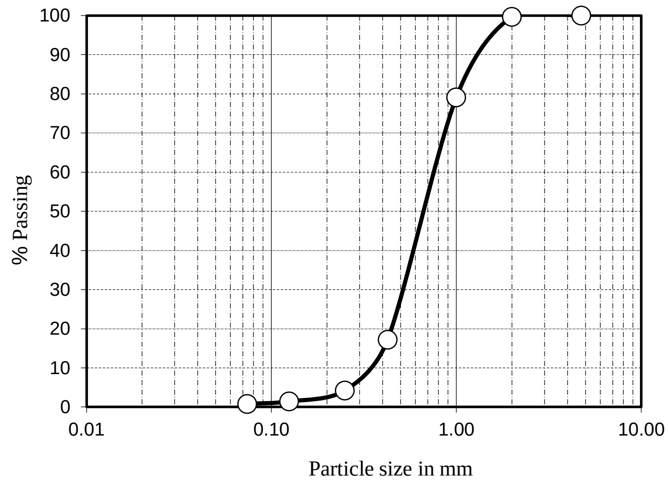

Figure 2. Particle size distribution of the subgrade.

Table 1. Properties of the sand subgrade

Properties	Value
D_{10} (mm)	0.36
D_{30} (mm)	0.55
D_{60} (mm)	0.76
Coefficient of uniformity, C_u	2.11
Coefficient of curvature, C_c	1.11
Specific gravity	2.74
Maximum dry density (kN/m^3)	16.57
Minimum dry density (kN/m^3)	14.12
Minimum void ratio, e_{min}	0.62
Maximum void ratio, e_{max}	0.94
Relative density (%)	80

2.2. Palm tree pruning waste (PTPW)

Tensile test series were performed on PTPW samples with total length of 200 mm and span length of 100 mm. The tests were carried out at the speed of 1 mm/min and a photograph of the tensile test of PTPW is shown in Figure 3. Properties of PTPW are shown in Table 2.

Table 2. Properties of PTPW.

Properties	Units	Value
Material composition	-	Mexican fan palm
Average tensile strength	kN/mm^2	2.7
Water content	%	13
Thickness	mm	0.4

Figure 3. Tensile test procedure.

The photograph of the tailored and intact PTPW was shown in Figure 4. Tailored PTPW samples were prepared with no rips and discontinuities; therefore, PTPW samples were cut in a circular form, i.e., a diameter of 600 mm.

Figure 4. Intact and tailored PTPW.

2.3. Geotextile

Geotextile samples were cut the same dimension as tailored PTPW samples to provide same conditions in the experiments. Properties of geotextile which is fabricated from polypropylene (PP) are shown in Table 3.

Table 3. Properties of geotextile.

Properties	Units	Value
Material composition	-	Polypropylene (PP), white
Material density	g/cm^2	250
Tensile strength, md/cmd*	kN/m	13 / 15
Elongation at break	%	50
Static puncture strength	N	2500
Dynamic puncture strength	mm	20
Liquid permeability	m/s	0.06
Apparent opening	mm	0.12
UV resistance	%	70

*md = machine direction, cmd = cross machine direction

2.4. Experimental schedule

A wooden test box of 1 m × 1 m × 0.6 m (length, width, and height, respectively) was used in the cyclic loading experiments. The photograph of the test box and cyclic loading system are shown in Figure 5. A circular steel plate with 15 mm thick and 200 mm in diameter was used as the loading plate. To avoid the boundary effects, the loading plate was selected in the manner that its diameter equivalent to 1/5 of the width of the test box according to studies reported in the literature (Nair & Latha, 2016; Palmeira & Antunes, 2010). The loading plate was exactly located at the center and top of the sand bed. Vertical deformations of the loading plate were measured with two linear variable differential transformer (LVDT) placed on either side of the loading plate. In this study, the average deformations of the loading plate, which is measured with LVDTs, were used in the calculations. Due to the repetition of cyclic loading, the sand subgrade under the loading plate is subjected to two different vertical deformations which are resilient (elastic) and permanent (plastic) deformations. For a load cycle, while elastic deformation is the reversible section of the total deformation, plastic deformation is the non-reversible section of the total deformation. Resilient and permanent deformations were calculated at each load repetition individually. The calculation methodology is shown in Figure 6.

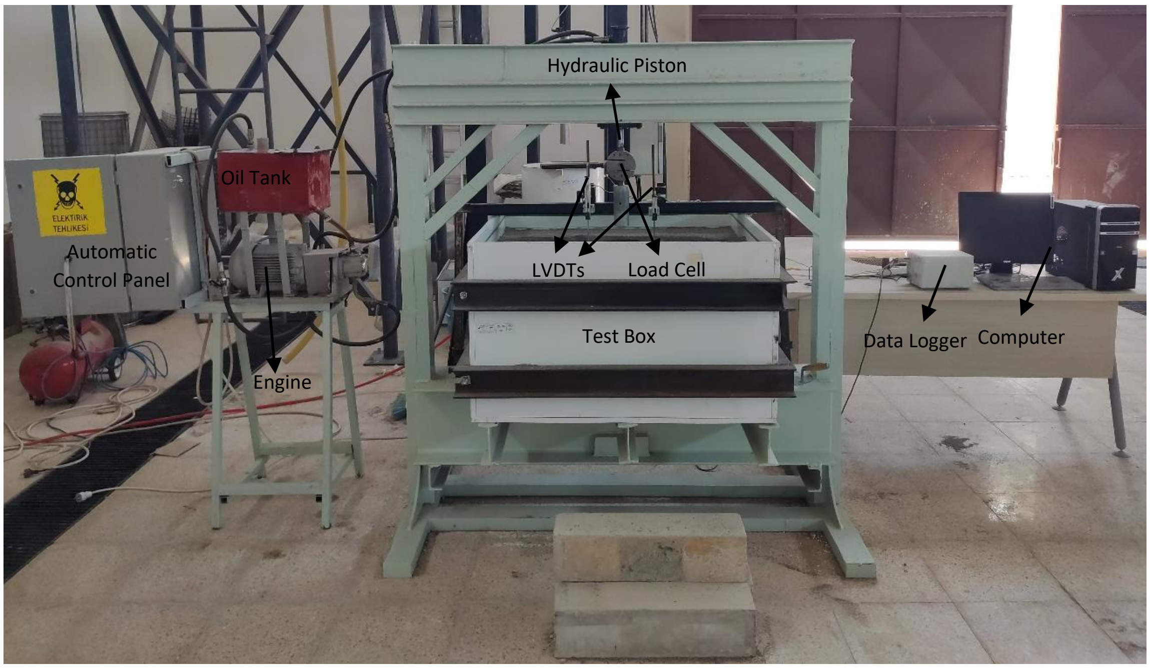

Figure 5. Test box and cyclic loading system.

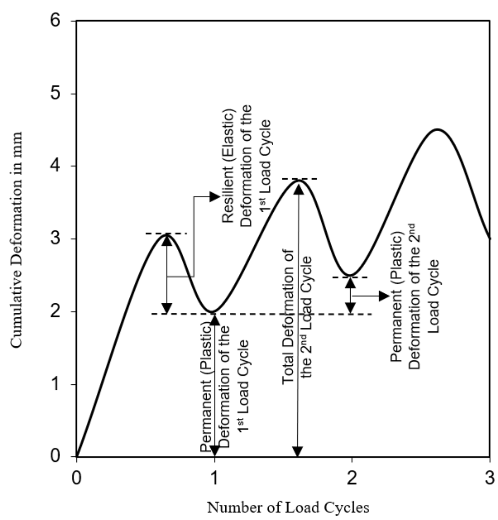

Figure 6. Calculation methodology of the deformation types.

The cyclic loading curve with a frequency of 1 Hz is illustrated in Figure 7. As evident from Figure 7, the cyclic loading curve has two-phase which are the loading and resting phase. In the first phase of the curve (i.e., loading phase), the load increases from zero to peak load at a magnitude of 225 kPa in 0.15 seconds and decreases to zero in 0.15 seconds. Thus, the loading phase is completed in 0.3 seconds. The resting phase is the stage in which the load is resting for 0.7 seconds. With the completion of the loading and resting phase, one loading cycle is applied to the loading plate in 1.0 seconds. In all experiments, the cyclic loading was applied to the plate for 5000 load cycles.

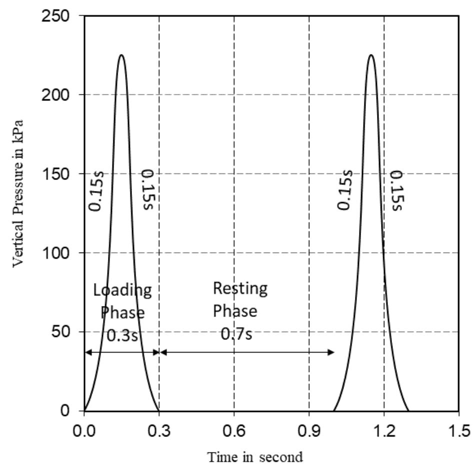

Figure 7. Cyclic loading curve.

Table 4. Experimental program.

Exp. No	Reinforcement type	Height of the subgrade (mm)	Burial depth (u) of reinforcement (mm)
1	Unreinforced (UR)	500	N/A
2	PTPW-reinforced (PTPWR-5)	500	50
3	Geotextile-reinforced (GR-5)	500	50
4	PTPW-reinforced (PTPWR-10)	500	100
5	Geotextile-reinforced (GR-10)	500	100
6	PTPW-reinforced (PTPWR-5-10)	500	50 and 100
7	Geotextile-reinforced (GR-5-10)	500	50 and 100

A series of tests were conducted to investigate the usability of PTPW as an alternative to commercially manufactured geotextile for soil improvement. The experimental program is shown in Table 4. In order to reach 80% relative density, the sand, which is the subgrade material, was compacted for every 100 mm height with the help of a circular vibratory plate. The first test was performed on the unreinforced subgrade to compare the performance of PTPW and geotextile-reinforced subgrades. The second and third tests were carried out to evaluate the performance of PTPW and geotextile reinforcements at a burial depth of 50 mm. Because to prevent any damage to geosynthetic material due to increasing number of cycles, the minimum burial depth was determined as 50 mm as suggestions of Suku, Prabhu, & Sivakumar Babu (2017). Similarly, whereas the fourth and fifth tests were conducted with PTPW and geotextile reinforcements at a burial depth of 100 mm, the last two tests were conducted with the reinforcements at both 50 mm and 100 mm burial depths. Schematic sketches of the PTPW and geotextile reinforcements are shown in Figure 8.

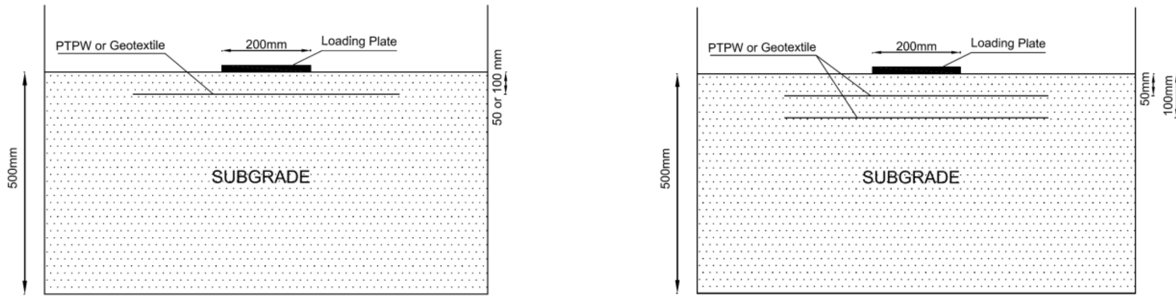

Figure 8. Schematic sketches of the experiments.

3. Experimental results and analysis

In this section, the experimental results of cyclic loading were superimposed on the figures for evaluation and comparison purposes. The results were evaluated according to total deformation, resilient deformation, percentage of resilient deformation, resilient modulus (M_R), permanent deformation, Rut Depth Reduction (RDR), and Traffic Benefit Ratio (TBR).

3.1. Total and Permanent Deformations

Total and permanent deformations of PTPW-reinforced, geotextile-reinforced and unreinforced subgrades versus the number of load cycles are presented in Figures 9 and 10, respectively. It is clearly understood from the figures that total and permanent deformations increase with the increasing number of load cycles. Total and permanent deformations are dominant at the initial loading cycles; nevertheless, it was observed that as the number of loading cycles increases, the rate of increase of these deformations decreases dramatically. As evident from the figures, total and permanent deformations of all the reinforced subgrades are lower than the unreinforced case at the end of all loading cycles. When the PTPW-10 and GR-10 subgrades are assessed between each other in terms of total and permanent deformations, it was realized that the results are nearly identical. Furthermore, the GR-5 subgrade outperformed the PTPWR-5 subgrade in the sense of total and permanent deformation. Similarly, considering the PTPWR-5-10 and GR-5-10, the PTPWR-5-10 subgrade showed higher deformation than the GR-5-10 regarding total and permanent deformations.

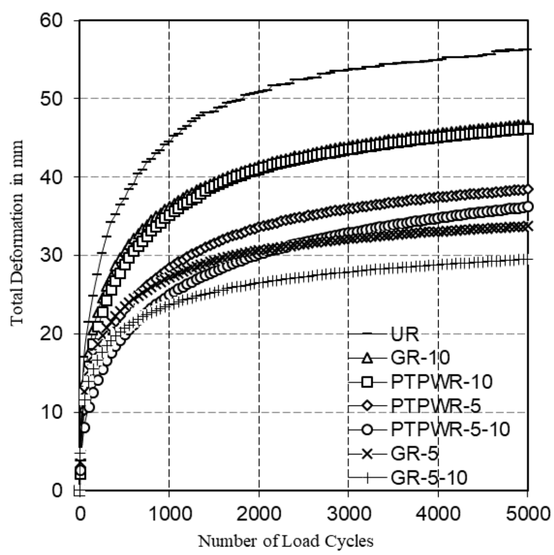

Figure 9. Total deformation versus number of loading cycles.

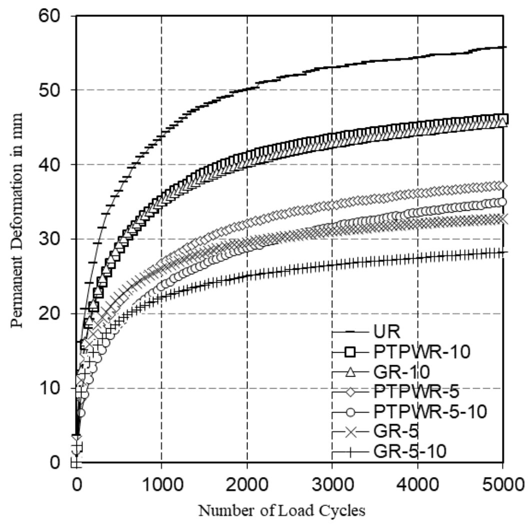

Figure 10. Permanent deformation versus number of loading cycles.

3.2. Traffic Benefit Ratio

The advantage of the use of PTPW and geotextile as a reinforcement agent and the evaluation of the performance improvement of the road foundation can be assessed by utilizing TBR used as a performance indicator of rutting behavior. TBR is described as the ratio of the number of load cycles of a reinforced subgrade section to that of an unreinforced case required to achieve the same permanent deformation. TBR values were evaluated according to the permanent deformations at the end of 5000 loading cycles and presented in Figure 11. It can be clearly observed from Figure 11 that TBR values of the PTPWR-5-10 subgrade are higher than the GR-5-10 subgrade till 20 mm permanent deformation, which provides to make a significant suggestion that when PTPW used as a reinforcement agent, it can be an alternative to commercially manufactured geotextile. Nevertheless, after the 20 mm permanent deformation, TBR values of the PTPWR-5-10 subgrade started to become lower than the GR-5-10 subgrade. Similar behavior was detected from the figure for PTPWR-5 and GR-5; however, the transition point is approximately at 25 mm permanent deformation at this stage. It is worth noting that the PTPWR-5 subgrade showed higher TBR values than the GR-5-10 till nearly 13 mm permanent deformation. When TBRs of the PTPWR-10 and GR-10 subgrades at 100 mm burial depth were assessed, it is significant to state that almost the same performance was observed regardless of reinforcement type.

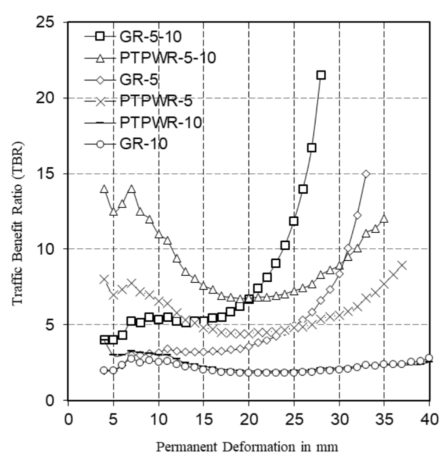

Figure 11. Variation of TBR with permanent deformation.

3.3. Ruth Depth Reduction

In this study, the RDR parameter was used to calculate the reduction in rutting behavior obtained by the PTPW and geotextile reinforcements. RDR is defined as the ratio of difference among cumulative permanent deformation (CPD) of reinforced and unreinforced subgrade to that of unreinforced subgrade for a certain number of cycles (Saride, Rayabharapu & Vedpathak, 2015). For N=nth load cycle, RDR can be defined as:

$$(RDR)_{N=n} = \left(1 - \frac{CPD_{unreinforced}}{CPD_{reinforced}}\right)_{N=n} \times 100 \qquad (1)$$

The RDR values were calculated for each 50 loading cycles for the entire PTPW and geotextile-reinforced subgrades in accordance with Equation 1 till the end of the 5000 loading cycles and presented in Figure 12. It can be observed from the figure that the RDR values of PTPW-reinforced subgrades reduced with the increasing number of loading cycles; in contrast, RDR values of geotextile-reinforced subgrades increased with the number of loading cycles. It can be inferred from this behavior that PTPW is superior in reducing the rutting at the initial loading cycles when compared to geotextile. Furthermore, similar behavior has been observed as with the TBR that initially, PTPW-reinforced subgrades performed higher RDR values than geotextile-reinforced subgrades until a specific number of loading cycles; nonetheless, after a transition point, RDR values have converged to a constant value. If the overall performance of the reinforced subgrades is evaluated in terms of RDR, GR-5-10 subgrade presented the highest RDR (49.31%) subsequently GR-5 (41.16%), PTPWR-5-10 (37.35%), PTPW-5 (33.18%), GR-10 (17.95%), and PTPWR-10 (17.08%).

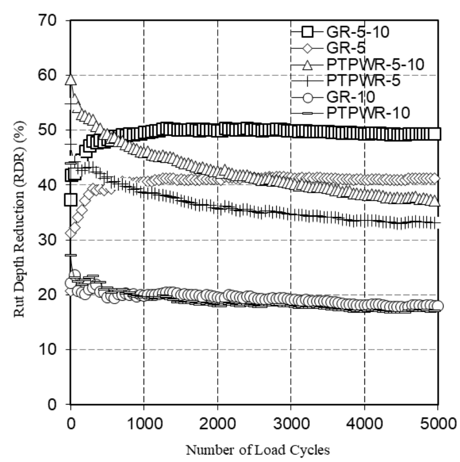

Figure 12. Rut depth reduction versus number of loading cycles.

3.4. Elastic Deformation

Elastic deformation curves of unreinforced and reinforced subgrades calculated for every loading cycle are illustrated in Figure 13. The calculation methodology of the elastic deformation for each loading cycle was given in the earlier section and presented in Figure 6. The general trend of all the elastic deformation curves indicates that with the increasing loading cycles, elastic deformations decrease and stabilize to nearly a constant value. It can be obviously seen from the figure that elastic deformations of the unreinforced subgrade have the minimum values as compared with reinforced cases. PTPWR-5 and GR-5-10 subgrades showed almost the same and the highest elastic deformations, followed by PTPWR-5-10, GR-10, GR-5, and PTPWR-10. It can be also inferred from this behavior that PTPW is a superior ability to increase elastic deformation in contrast to geotextile meaning that the higher elastic deformation occurs, the longer the service life of pavements is provided.

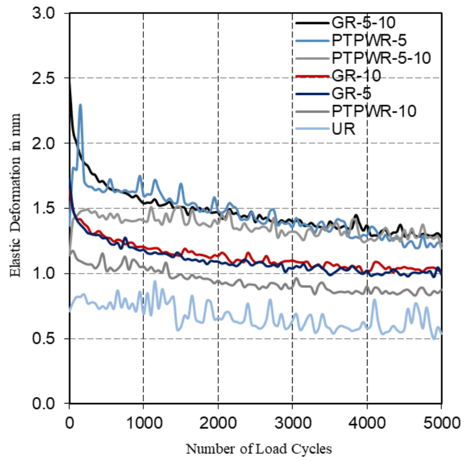

Figure 13. Elastic deformations versus number of loading cycles.

3.5. Percentage of elastic deformation

The percentage of elastic deformation is described as the rate of the elastic deformation to the total deformation at each load cycle. The percentage of elastic deformation of unreinforced and reinforced subgrades is shown in Figure 14. It can be clearly seen from the figure that the percentage of elastic deformations of reinforced and unreinforced increased swiftly during initial loading cycles; however, converged rapidly to a constant value with the increasing number of loading cycles. It is apparent that as expected, the unreinforced subgrade had the lowest value of percentage of elastic deformation compared to the reinforced subgrades meaning that elastic behavior of all reinforced subgrades was enhanced by the hep of reinforcement; thus, it can be said that an increase in the service life of the pavement is provided.

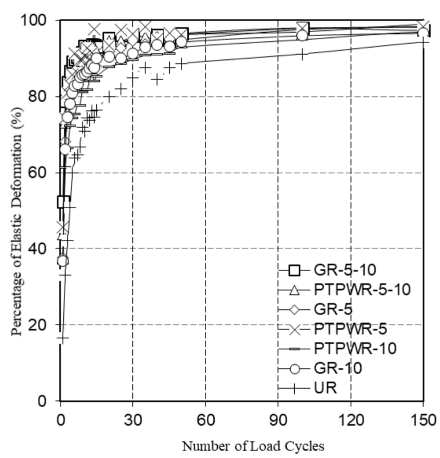

Figure 14. Percentage of elastic deformation versus number of loading cycles.

3.6. Resilient modulus

In the current study, a functional method put forward by (Qian, Han, Pokharel, & Parsons, 2011) was made use of so as to calculate M_R values based on the back-calculation of the M_R from the resilient deformation results of all experiments, and this method was given in Equation 2.

$$\delta = \frac{Blq(1 - v^2)}{E} \qquad (2)$$

Where, δ is the resilient deformation of any load cycle, B is the diameter of the loading plate, I is the influence factor (taken as an average of 2 at the center and 1.2 at the edge of the plate (Ahlvin & Ulery, 1962)) q is the applied pressure on loading plate, ν is the poisons ratio, E is the modulus of elasticity (i.e., M_R). M_R values of reinforced and unreinforced subgrades are superimposed on Figure 15 for comparison purposes. It is apparent from the figure that M_R values of the unreinforced subgrade are greater than PTPW-reinforced and geotextile-reinforced cases. It ought not to be taken into consideration as a drawback because higher elasticity makes a major contribution to enhance the service life of pavements. Moreover, this behavior is in line with much research in the literature (Nair & Latha, 2016; Pokharel, Han, Leshchinsky & Parsons, 2018; Tafreshi, Khalaj, & Dawson, 2014; Thakur, Han, Pokharel, & Parsons, 2012).

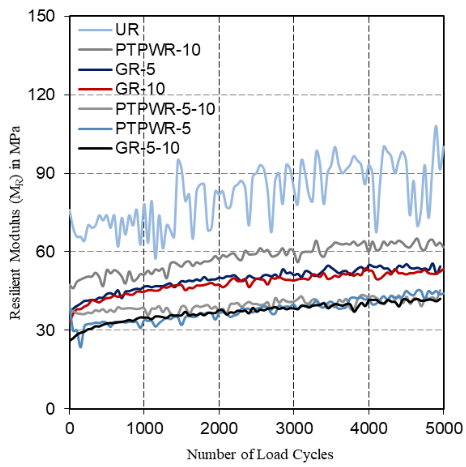

Figure 15. Resilient modulus versus number of loading cycles.

4. Conclusions and comments

This paper presents a series of cyclic loading tests to evaluate the performance of palm tree pruning waste (PTPW) as a soil improvement agent. This study provides a benchmark of commercially manufactured geotextile versus PTPW which is a waste material. The results were assessed with regards to total deformation, resilient deformation, percentage of resilient deformation, resilient modulus (M_R), permanent deformation, rut depth reduction (RDR), and traffic benefit ratio (TBR). The following conclusions can be drawn obtained from this experimental study:

1. PTPW and geotextile-reinforced subgrades outperformed significantly compared to the unreinforced subgrade in terms of total deformation, permanent deformation, elastic deformations, and percentage of elastic deformation.
2. PTPW-reinforced subgrades have a higher value of TBR and RDR at the initial loading cycles compared to the geotextile-reinforced subgrades.
3. Geotextile and PTPW significantly decreased the rut depth at the rate of 49.31 % and 37.15 % at the end of 5000 load cycle, respectively meaning that PTPW, which is a natural and waste material, provided an opportunity to be used as novel and eco-friendly solution to improve rutting behavior of soil.
4. TBR values obtained from the most effective cases of geotextile and PTPW-reinforced subgrades were approximately similar at 20 mm permanent deformation (i.e., 6.71 and 6.76, respectively).
5. With the inclusion of PTPW and geotextile, elastic deformation increased dramatically; moreover, more elastic behavior was observed when PTPW was used as soil improvement agent.
6. Taking into account all of these, it can be concluded that the results of geotextile and PTPW-reinforced subgrades were similar to each other; therefore, PTPW, which is a waste material, can be used instead of commercially manufactured geotextile to improve rutting performance of the soil.

Author contributions: The contribution of the authors is equal.

Acknowledgments: We would like to thank GEOPLAS company for their support in supply of geotextile.

Conflicts of interest: Authors have declared no conflict of interest.

References

Abdeldjouad, L., Asadi, A., Ball, R. J., Nahazanan, H., & Huat, B. B. K. (2019). Application of alkali-activated palm oil fuel ash reinforced with glass fibers in soil stabilization. Soils and Foundations, 59(5), 1552–1561.

Ahlvin, R. G., & Ulery, H. H. (1962). Tabulated values for determining the complete pattern of stresses, strains, and deflections beneath a uniform circular load on a homogeneous half space. Highway Research Board Bulletin, (342).

Altay, G., Kayadelen, C., Canakci, H., Bagriacik, B., Ok, B., & Oguzhanoglu, M. A. (2021). Experimental investigation of deformation behavior of geocell retaining walls. Geomechanics and Engineering, Vol. 27, No. 5, 419-431

Altay, G., Kayadelen, C., Taskiran, T., Bagriacik, B., & Toprak, O. (2021). Frictional properties between geocells filled with granular material. Revista de la construcción, 20(2), 332-345.

Altay, G., Kayadelen, C., Taşkıran, T., & Kaya, Y. Z. (2019). A laboratory study on pull-out resistance of geogrid in clay soil. Measurement, 139, 301-307.

Arifin, Y. F., & Rahman, G. (2019). Stabilization of Soft Soil with Cement and Palm Kernel Shell Ash Admixture. MATEC Web of Conferences, 280, 04011.

Basha, E. A., Hashim, R., Mahmud, H. B., & Muntohar, A. S. (2005). Stabilization of residual soil with rice husk ash and cement. Construction and Building Materials, 19(6), 448–453.

Bhattacharyya, R., Fullen, M. A., Davies, K., & Booth, C. A. (2009). Utilizing palm-leaf geotextile mats to conserve loamy sand soil in the United Kingdom. Agriculture, Ecosystems and Environment, 130(1–2), 50–58.

Cuelho, E. V., & Perkins, S. W. (2017). Geosynthetic subgrade stabilization – Field testing and design method calibration. Transportation Geotechnics, 10, 22–34.

Evangeline, S. Y., Sayida, M. K., & Girish, M. S. (2019). Long-Term Performance of Rural Roads Reinforced with Coir Geotextile – A Field Study. Journal of Natural Fibers, 1–18.

Fannin, R. J., & Sigurdsson, O. (1996). Field Observations on Stabilization of Unpaved Roads with Geosynthetics. Journal of Geotechnical Engineering, 122(7), 544–553.

Ferrández-García, C.-E., Ferrández-García, A., Ferrández-Villena, M., Hidalgo-Cordero, J., García-Ortuño, T., & Ferrández-García, M.-T. (2018). Physical and Mechanical Properties of Particleboard Made from Palm Tree Prunings. Forests, 9(12), 755.

Garcia-Ortuno, T., Ferrandez Garcia, M. T., Andreu Rodriguez, J., Ferrandez Garcia, C. E., & Ferrandez-Villena, M. (2011). Evaluating the properties of palm particle boards (Washingtonia robusta H. Wendl). In Proceedings of the 6th Iberian Congress of Agroengineering, 126–130.

George, A. M., Banerjee, A., Puppala, A. J., & Saladhi, M. (2021). Performance evaluation of geocell-reinforced reclaimed asphalt pavement (RAP) bases in flexible pavements. International Journal of Pavement Engineering, 22(2), 181–191.

Gil-Lopez, T., Medina-Molina, M., Verdu-Vazquez, A., & Martel-Rodriguez, B. (2017). Acoustic and economic analysis of the use of palm tree pruning waste in noise barriers to mitigate the environmental impact of motorways. Science of the Total Environment, 584–585, 1066–1076.

Giroud, J. P., & Han, J. (2004). Design Method for Geogrid-Reinforced Unpaved Roads. I. Development of Design Method. Journal of Geotechnical and Geoenvironmental Engineering, 130(8), 775–786.

Gray, D. H., & Ohashi, H. (1983). Mechanics of Fiber Reinforcement in Sand. Journal of Geotechnical Engineering, 109(3), 335–353.

Hausmann, M. R. (1987). Geotextiles for unpaved roads-A review of design procedures. Geotextiles and Geomembranes, 5(3), 201–233.

Kayadelen, C., Önal, T. Ö., & Altay, G. (2018). Experimental study on pull-out response of geogrid embedded in sand. Measurement, 117, 390-396.

Mamatha, K. H., & Dinesh, S. V. (2019). Performance evaluation of geocell-reinforced pavements. International Journal of Geotechnical Engineering, 13(3), 277–286.

Mandal, I., & Pal, S. (2020). COVID-19 pandemic persuaded lockdown effects on environment over stone quarrying and crushing areas. Science of the Total Environment, 732, 139281.

Marandi, S. M., Bagheripour, M. H., Rahgozar, R., & Zare, H. (2008). Strength and ductility of randomly distributed palm fibers reinforced silty-sand soils. American Journal of Applied Sciences, 5(3), 209–220.

Mujah, D., Rahman, M. E., & Zain, N. H. M. (2015). Performance evaluation of the soft soil reinforced ground palm oil fuel ash layer composite. Journal of Cleaner Production, 95, 89–100.

Nair, A. M., & Latha, G. M. (2016). Repeated load tests on geosynthetic reinforced unpaved road sections. Geomechanics and Geoengineering, 11(2), 95–103.

Negi, M. S., & Singh, S. K. (2019). Experimental and numerical studies on geotextile reinforced subgrade soil. International Journal of Geotechnical Engineering, 1–12.

Nnochiri, E. S., Ogundipe, O. M., & Oluwatuyi, O. E. (2017). Effects of Palm Kernel Shell Ash on Lime-Stabilized Lateritic Soil. Slovak Journal of Civil Engineering, 25(3), 1–7.

Önal, Y. (2021). Geosentetiklerle güçlendirilmiş karayolu temel tabakasının davranışının tekrarlı yükler altında incelenmesi. Thesis (MSc). Osmaniye Korkut Ata University, Osmaniye, Turkey.

Palmeira, E. M., & Antunes, L. G. S. (2010). Large scale tests on geosynthetic reinforced unpaved roads subjected to surface maintenance. Geotextiles and Geomembranes, 28(6), 547–558.

Pokharel, S. K., Han, J., Leshchinsky, D., & Parsons, R. L. (2018). Experimental evaluation of geocell-reinforced bases under repeated loading. International Journal of Pavement Research and Technology, 11(2), 114–127.

Pokharel, S. K., Han, J., Leshchinsky, D., Parsons, R. L., & Halahmi, I. (2010). Investigation of factors influencing behavior of single geocell-reinforced bases under static loading. Geotextiles and Geomembranes, 28(6), 570–578.

Pourakbar, S., Asadi, A., Huat, B. B. K., & Fasihnikoutalab, M. H. (2015). Stabilization of clayey soil using ultrafine palm oil fuel ash (POFA) and cement. Transportation Geotechnics, 3, 24–35.

Qian, Y., Han, J., Pokharel, S. K., & Parsons, R. L. (2011). Determination of Resilient Modulus of Subgrade Using Cyclic Plate Loading Tests. 4743–4751.

Qu, J., & Xiong, K. (2020). Influences of Curing Environment on Strength Performances of Shanghai Clayey Soil Reinforced with Palm Fiber. Advances in Civil Engineering.

Qu, J., & Zhao, D. (2016). Stabilising the cohesive soil with palm fibre sheath strip. Road Materials and Pavement Design, 17(1), 87–103.

Qu, J., & Zhu, H. (2021). Function of palm fiber in stabilization of alluvial clayey soil in Yangtze River Estuary. Journal of Renewable Materials, 9(4), 767–787.

Rashidian, V., Naeini, S. A., & Mirzakhanlari, M. (2018). Laboratory testing and numerical modelling on bearing capacity of geotextile-reinforced granular soils. International Journal of Geotechnical Engineering, 12(3), 241–251.

Saride, S., Rayabharapu, V. K., & Vedpathak, S. (2015). Evaluation of Rutting Behaviour of Geocell Reinforced Sand Subgrades Under Repeated Loading. Indian Geotechnical Journal, 45(4), 378–388.

Shukla, S. K. (2002). Geosynthetics and their Applications. In Geosynthetics and their Applications.

Singh, M., Trivedi, A., & Shukla, S. K. (2019). Strength enhancement of the subgrade soil of unpaved road with geosynthetic reinforcement layers. Transportation Geotechnics, 19, 54–60.

Suku, L., Prabhu, S. S., Ramesh, P., & Babu, G. L. S. (2016). Behavior of geocell-reinforced granular base under repeated loading. Transportation Geotechnics, 9, 17–30.

Suku, L., Prabhu, S. S., & Sivakumar Babu, G. L. (2017). Effect of geogrid-reinforcement in granular bases under repeated loading. Geotextiles and Geomembranes, 45(4), 377–389.

Tafreshi, S. N. M., Khalaj, O., & Dawson, A. R. (2014). Repeated loading of soil containing granulated rubber and multiple geocell layers. Geotextiles and Geomembranes, 42(1), 25–38.

Thakur, J. K., Han, J., Pokharel, S. K., & Parsons, R. L. (2012). Performance of geocell-reinforced recycled asphalt pavement (RAP) bases over weak subgrade under cyclic plate loading. Geotextiles and Geomembranes, 35, 14–24.

Zhang, L., Zhao, M., Shi, C., & Zhao, H. (2010). Bearing capacity of geocell reinforcement in embankment engineering. Geotextiles and Geomembranes, 28(5), 475–482.